Geomorphology 354 (2020) 107044

Contents lists available at ScienceDirect

Geomorphology

journal homepage: www.elsevier.com/locate/geomorph

Geochronology and evolution of a complex barrier, Younghusband Peninsula, South Australia

Sergio R. Dillenburg [a,e,*], Patrick A. Hesp [b], Robert Keane [b], Graziela Miot da Silva [b], André O. Sawakuchi [c], Ian Moffat [d], Eduardo G. Barboza [a,e], Volney J.B. Bitencourt [e]

[a] Universidade Federal do Rio Grande do Sul, Instituto de Geociências, Centro de Estudos de Geologia Costeira e Oceânica, Av. Bento Gonçalves 9500, Porto Alegre, RS 91509-900, Brazil
[b] Beach and Dune Systems (BEADS) Laboratory, College of Science and Engineering, Flinders University, Sturt Road, Bedford Park, South Australia, 5041, Australia
[c] Universidade de São Paulo, Instituto de Geociências, Rua do Lago 562, São Paulo, SP 05508-080, Brazil
[d] Archaeology, College of Humanities and Social Sciences, Flinders University, Sturt Road, Bedford Park, South Australia 5041, Australia
[e] Universidade Federal do Rio Grande do Sul, Instituto de Geociências, Programa de Pós-Graduação em Geociências, Av. Bento Gonçalves 9500, Porto Alegre, RS 91509-900, Brazil

ARTICLE INFO

Article history:
Received 18 July 2019
Received in revised form 13 January 2020
Accepted 15 January 2020
Available online 16 January 2020

Keywords:
Foredune ridges
Barrier progradation
The Granites
OSL dating

ABSTRACT

This study examines the southeastern end of the Younghusband Peninsula in South Australia at a location called The Granites in order to gain a better understanding of the processes of formation of the foredune ridge system, and to investigate the drivers that controlled its progradational development during the Holocene. Our findings are based on a morphological analysis, a ground penetrating radar survey, and ^{14}C and OSL dating. The Younghusband Peninsula at The Granites was formed by an initial aggradational phase resulting in a single complex foredune ridge, and which ended around 4.3 ka, and by a regressive (progradational) barrier phase (750 m wide) that developed in the last 4.3 ka, under very low rates of progradation (0.38 to 0.09 m/yr). The last part of this phase shows significant foredune ridge building in the last 1000 years or so. Barrier progradation via foredune ridge development is likely an effect driven by low wave energy that favored conditions for coastal stability and foredune formation. Paleontological and GPR data indicate a maximum sea-level of +1.23 to +1.5 m, respectively, during initial barrier development. The foredune ridge plain of the barrier experienced at least three phases of significant aeolian activity with ages centered at around 3.9, 3.4 and 3.0 ka suggesting their occurrence at 500 to 400-year events. Computer modelling indicates that sediments for the progradational phase of the barrier were provided by the forced regression produced by a sea-level fall over the past 4.3 ka. The large foredune complex formed during the last phase of progradation could be the result of both the very low progradation rate of 0.09 m/yr, and periods of disturbance possibly related to enhanced storm activity.

1. Introduction

In most cases the morphological and stratigraphic type of barrier that occurs along a coast is controlled by wave and tide energy, past and present sea-level oscillations, geological inheritance, and sediment availability (Short and Hesp, 1982; Roy et al., 1994; Dillenburg and Hesp, 2009). These factors vary considerably from one coast to another, and even along a single stretch of coast. For example, in the case of southern Brazil, a 750 km long and gently undulating stretch of coast exists and comprises a continuous barrier system that alternates between progradational (regressive), aggradational (stationary) and retrogradational (transgressive) barriers, driven by variations in wave energy and coastline orientation (Dillenburg et al., 2000, 2006, 2009).

Many coastal barriers tend to one of the three major types, that is, either progradational, aggradational or retrogradational if one uses, for example, Morton's (1994) classification of barriers. While the 'Australian' classification of barriers includes other types reflecting their surficial morphology (e.g. transgressive dunefield barriers), the dominant common types are the same as those of Morton's classification (Roy et al., 1980; Thom, 1984). A complex barrier is a barrier which comprises two different types (e.g. progradational and retrogradational) or displays two distinct surficial morphologies (e.g. relict foredune plain and transgressive dunefield; Curray et al. (1969), McKee (1979); Hesp et al. (2009). While some examples of complex barriers exist in the literature (e.g. Rodriguez and Meyer, 2006; Hesp et al., 2009; Timmons et al., 2010; Dillenburg et al., 2017) it is still unusual to find studies of such complex barriers.

The Sir Richard and Younghusband peninsulas are separated by the mouth of the Murray River and comprise a Holocene barrier which is 190 km long, in the form of a NW-SE orientated gentle arc (Fig. 1). The emerged part of the barrier is mostly <2 km wide, and has a

* Corresponding author at: Universidade Federal do Rio Grande do Sul, Instituto de Geociências, Programa de Pós-Graduação em Geociências. Av. Bento Gonçalves 9500, Porto Alegre, RS 91509-900, Brazil.
E-mail address: sergio.dillenburg@ufrgs.br (S.R. Dillenburg).

https://doi.org/10.1016/j.geomorph.2020.107044
0169-555X/

morphology dominated by transgressive dunefields and parabolic dunes, except for the last 40 km to the southeast, where the presence of a narrow, prograded foredune ridge plain indicates the barrier is a regressive barrier. This barrier is the longest continuous barrier in Australia, and despite its ecological and geomorphological significance, the geological formation and evolution of the barrier during the Holocene is still poorly understood. Up to now the barrier was specifically studied only in regard to the morphodynamics of its beaches and surfzone-beach-dune interactions (Short and Hesp, 1984; Hesp, 1988a), offshore and shelf evolution (Hill et al., 2009), excavations and dating of some archaeological sites (Luebbers, 1978, 1982; Bourman and Murray-Wallace, 1991; Bourman et al., 2000), evolution of the Murray mouth region during the Quaternary and in historical times (Murray-Wallace et al., 2010; Bourman et al., 2016), a general analysis of Holocene coastal evolution of a small portion of the northern part of the barrier system (Harvey et al., 2006), the general description of Holocene foredune ridges formed at The Granites in the last 7 ka (Murray-Wallace, 2018), historical changes in vegetation cover in the northern portion (Moulton et al., 2018), and the influence of invasive vegetation on the morphological development of foredunes (Hilton and Harvey, 2002).

This study examines one portion of the southeastern end of the Younghusband Peninsula (henceforth, YP), at an area termed "The Granites" (Figs. 1 and 2). At this site we conducted a morphological analysis of the foredune ridge plain and adjacent surfzone-nearshore utilizing satellite imagery and bathymetric maps, a ground penetrating radar survey of the plain, and ^{14}C and optically stimulated luminescence (OSL) dating of the lagoonal and ridge sediments in order to contribute to a better geological and geomorphological knowledge of this southernmost sector of the YP coastal barrier, and also to specifically investigate the drivers (e.g. sea-level, climate, wave energy) of the progradational development of this coastal sector.

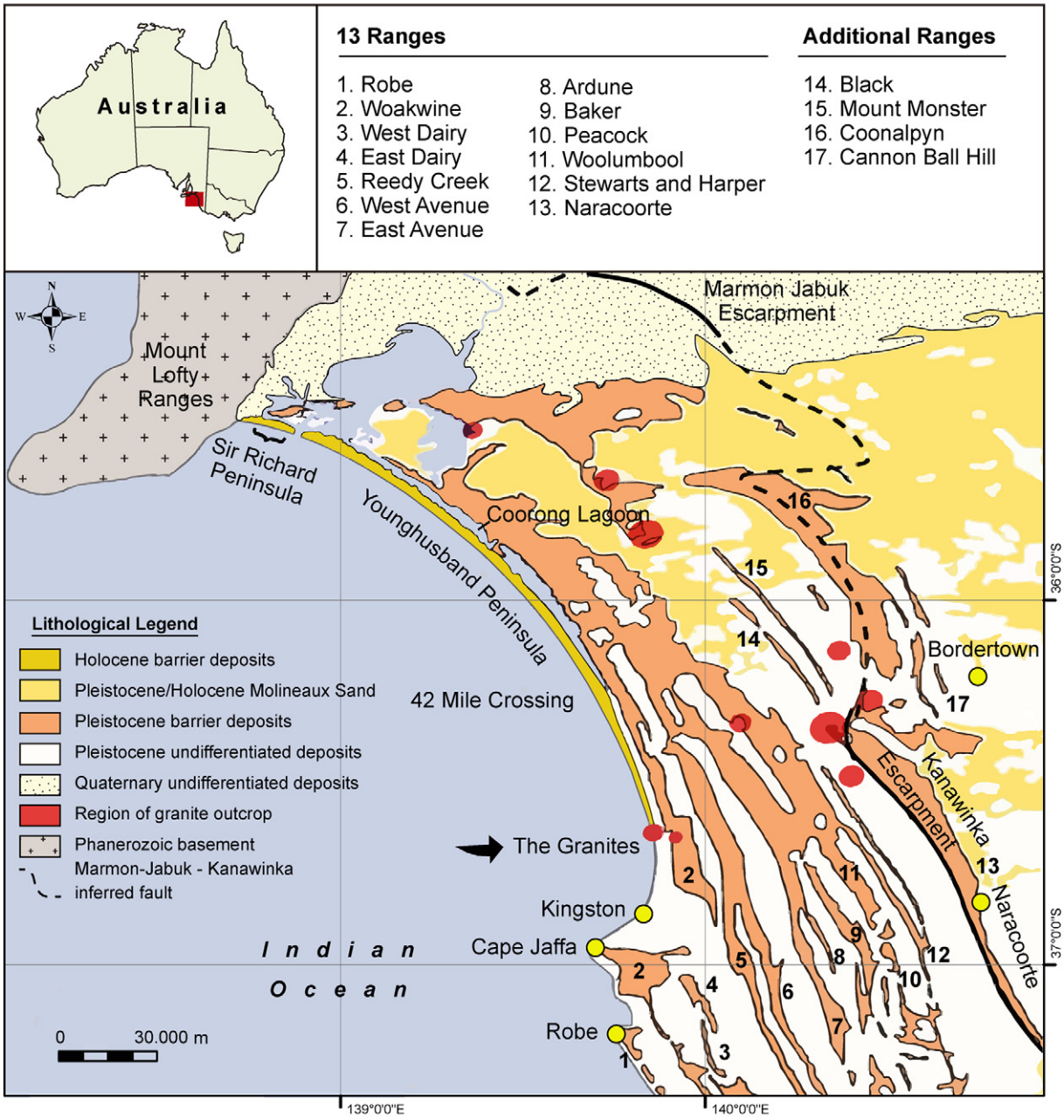

Fig. 1. Location of the Younghusband Peninsula, Coorong Lagoon, The Granites study area, and older Pleistocene barriers (modified from Bourman et al., 2018). Complementary Geology information from the Department for Energy and Mining, the Government of South Australia, sourced on 16 September, 2019.

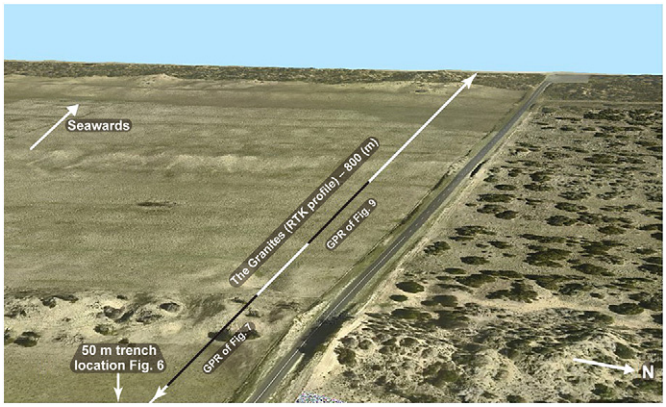

Fig. 2. Oblique lidar image of The Granites region showing variations in the height of foredune ridges across the barrier and the landward palaeo-Coorong lagoon flat (bottom left portion) (imagery acquired 22/5/2018 through 24/8/2018). The long white line locates 800 m of the RTK topographic profile of Fig. 3. The black lines locate the GPR profiles of Figs. 7 and 9.

2. Regional setting

2.1. The Younghusband Peninsula Regional Environment

The YP is a coastal barrier that occurs between the Murray River mouth and Cape Jaffa (Fig. 1). It is formed by carbonate-rich Holocene beach and dune sands, with a substrate partly comprising Pleistocene aeolian calcarenite barrier segments (Harvey et al., 2006). The Holocene barrier forms just the latest barrier in a massive multiple barrier sequence extending back into the Pliocene (Cook et al., 1977; Huntley et al., 1994; Murray-Wallace et al., 2001; Banerjee et al., 2003; Short and Woodroffe, 2009). The region encompassing Encounter Bay on which the YP occupies the eastern margin, experiences a microtidal (0.8 m) tide regime (Short and Hesp, 1984). The deep-water wave climate is high energy and wave height can exceed 5 m. Even though substantial attenuation across the shelf occurs, wave height can exceed 2 m 50% of the year (Short and Hesp, 1984; Provis and Steedman, 1985; Short, 1988). Reissen and Chappell (1991) analysed storm data for 3849 individual storms which could move sand in the 51 year period up to 1991, and found the maximum significant wave heights and corresponding period for waves approaching the Murray Mouth were west, 2 m and 12 s, southwest 5 m and 12 s, south 5 m and 12 s, and south and southeast, 4 m and 8 s.

Because the shelf width increases dramatically in the SE portion of the Bay, the YP surfzone-beach system ranges from a high wave energy, multi-bar, fine sand, dissipative surfzone-beach system in the NW portion, through a high wave energy, multi-bar and rip, intermediate surfzone-beach system with medium to coarse and shelly sand in the central region, to a low wave energy, very fine sand, dissipative surfzone-beach system in the SE portion. It thus has a significant gradient in wave energy, grain size and surfzone-beach type alongshore, without a significant change in orientation to dominant W-SW winds. Sands are predominantly carbonate sands derived from the shelf (Short and Hesp, 1984; Hesp, 1988a).

Transgressive dunefields comprising transverse and barchanoid dunes, large precipitation ridges, parabolic dunes and blowouts dominate the dunes of the YP and range up to 40 m in height above mean sea level (Moulton et al., 2018). Mobile dunes were extant prior to rabbit or other animal introductions in the region as the explorer Matthew Flinders noted significant drifting sand dunes in his 1802 report describing the YP, and recently reinforced by Moulton et al. (2018). The Coorong lagoon, which lies behind the YP, is a barrier lagoon/estuary system associated with the Murray River and is a Ramsar Wetland of International Importance. In the SE portion (towards Kingston) the barrier changes to a foredune plain. The barrier in toto is therefore classified as a complex barrier in the sense that the surface morphology of the barrier comprises two distinct types of coastal dune systems – in this case, parabolic/transgressive dunefields and foredune plains following definitions by Curray et al. (1969) and McKee (1979).

2.2. Holocene palaeo-sea levels and tectonics

Palaeo-sea levels in South Australia have primarily been determined from sites well up the Spencer Gulf or the Gulf St Vincent, 300 and 200 km to the northwest of the study area, respectively (e.g. Belperio et al., 2002). These data indicate sea level reached the present level at 8000 to 7500 years BP, rose no more than 1 m above, and likely fell in a relatively smooth fashion to the present level somewhere between 2000 years BP and the present (Lewis et al., 2013). In the YP/Coorong open ocean coastal region, sea level probably reached a high of +1.0 m 7000 years ago, based on the studies reviewed in Belperio et al. (2002). Oliver et al. (2019b) state that the Holocene high stand reached around +2 m in nearby Guichen Bay to the south of the YP study area. The YP region is also quite different compared to other dated transgressive dunefields in Australia because it displays a variable tectonic gradient alongshore. The SE margin towards The Granites is rising (uplift of 0.07 mm/yr), while the Murray mouth region is sinking at 0.02 mm/yr (Bourman et al., 2016). This tectonic activity has very likely occurred throughout the Holocene.

3. Methods

The data base of this research includes a bathymetric analysis of the adjacent inner continental shelf of the southern sector of YP, a detailed Real Time Kinematic (RTK) altimetric survey performed along a transverse profile at The Granites, a ground penetrating radar (GPR) survey performed along the RTK profile, and the collection of 17 samples from aeolian (foredune) deposits and four samples of mollusks with their shells still articulated (therefore probably in in-life positions) collected in a trench excavated in the backbarrier lagoonal/estuarine deposits for OSL dating and AMS ^{14}C dating, respectively.

3.1. Geomorphological analysis

The southern sector of YP was analysed using Google Earth Pro satellite images and a bathymetric map produced by the integration of a Base Map from ArcGIS and data from SRTM30 Plus (*http://topex.ucsd.edu/WWW_html/srtm30_plus.html*). At The Granites a detailed RTK altimetric survey was performed along a transverse profile. All altitude data could have a maximum error of 0.4 to 0.8 m, although a comparison of the RTK data with modern tide and sea level data during surveys indicate the error is smaller. The height data are referred to the Australia Height Datum (AHD) which is roughly mean sea level (0.0).

3.2. OSL and AMS ^{14}C dating

The OSL samples were collected from the base of a 1 m deep hole drilled with a hand auger, by the vertical (30 cm) insertion of a 6 cm diameter plumbing pipe, which was immediately capped and then covered with aluminum foil and black plastic after collection. Exceptions are samples 2.1, 2.2, 7.5, 9.5, 11.5 and 13 which were collected by horizontal insertion of a 12 or 15 cm long pipe into the side walls of dune ridges cut for road construction. The OSL dating was performed in the Gamma Spectrometry Laboratory (LEGaL), at the Geosciences Institute of the University of São Paulo (USP) in Brazil. OSL ages estimated were obtained on quartz grains extracted from 17 sand samples. Preparation of quartz concentrates followed standard procedures (Aitken, 1998) and included wet sieving to isolate the 180–250 μm grain size fraction followed by chemical treatments with hydrogen peroxide and

hydrochloric acid (10% HCl) to eliminate organic compounds and carbonates, respectively. Quartz grains (2.65 g/cm^3) were subsequently isolated from heavy minerals and feldspar using lithium metatungstate solutions at densities of 2.75 and 2.62 g/cm^3. Quartz concentrates were then treated with hydrofluoric acid (38% HF) for 40 min to eliminate the outer rind of grains affected by alpha radiation and remnant feldspars. A final treatment with HCl was performed to eliminate eventual precipitates formed during HF treatment. Equivalent doses were determined using the single-aliquot regenerative dose (SAR) protocol applied to multigrain aliquots of quartz (Murray and Wintle, 2003). Luminescence measurements were conducted in two Risø TL/OSL DA-20 systems equipped with ^{90}Sr/^{90}Y radiation sources delivering dose rates of 0.075 and 0.109 Gy/s (steel cups), Hoya U-340 filters for light detection in the ultraviolet band and blue LEDs for light stimulation. A dose recovery test was performed with quartz aliquots from sample Gran 2. Ten aliquots were bleached under a solar simulator lamp for 4 h. The calculated-to-given dose ratio was 1.00 ± 0.05 for a given dose of 1.75 Gy and preheat temperature of 200 °C. For each sample, 24 quartz aliquots were measured and only aliquots with a recycling ratio within 1.0 ± 0.1, recuperation <5% and negligible infrared stimulated luminescence signal were considered for equivalent dose calculation (Murray and Wintle, 2003). Equivalent doses were calculated using the Central Age Model (CAM) as proposed by Galbraith et al. (1999). Overdispersion (OD) of equivalent dose distributions was considered to evaluate bleaching prior to deposition and eventual post-depositional sediment mixture due to bioturbation. Dose rates were calculated through concentrations of uranium (U), thorium (Th) and potassium (K) and conversion factors outlined by Guérin et al. (2011). Radionuclides concentrations were measured through high-resolution gamma ray spectrometry using a high-purity germanium (HPGe, 55% relative efficiency) detector (Canberra Instruments) encased in an ultralow background shield. Samples were dried and stored in sealed plastic containers for at least 21 days for radon requilibration before gamma spectrometry. Cosmic dose rates were calculated according to Prescott and Hutton (1994). Age errors were calculated according to a gaussian law of error propagation.

The radiocarbon dating (AMS) was performed by Beta Analytic Inc. (Miami, Florida, USA). Prior to calibration the conventional ages were adjusted for local reservoir correction. The calibration curve of Reimer et al. (2013) was used. Three shells of bivalve mollusks (two of *Anapela cycladea* and one of *Katelysea scalarina*) found in in-life position (one valve of each was analysed) and three very well-preserved shells (not broken and no dissolution or crystallization signs) of a gastropod (*Tatea rufilabris*) were dated. The OSL and radiocarbon dating results are presented in Tables 1 and 2.

The ^{14}C datings are reported as radiocarbon years before present (e.g. 6700 yrs. BP or 6.7 ka BP), while OSL datings are simply reported as years or ka (e.g. 4300 yrs. or 4.3 ka).

3.3. GPR survey

Two lines of GPR survey were performed at The Granites utilizing a MALA Ground Explorer GPR device. Two antennas were utilized (GX160 and GX450 MHz). The first GPR transect extended from the backbarrier lagoon over the oldest and innermost ridge (115 m), and the other transect extended from the inner ridge to the back of the large relict foredune-blowout complex (750 m). Due to the poor quality of the longest (750 m) GPR data, only a short section is presented (see Fig. 2). Unfortunately, we were unable to collect reliable GPR records from the large relict foredune or the adjacent transect across the road and down to the beach due to irregular terrain conditions and thick vegetation. Altitudes were determined by a RTK system during the survey, and topographic correction was applied. A dielectric constant of 6 for wet sand was used to convert travel-time to depth, which represents a velocity of 0.12 m/ns (Davis and Annan, 1989). The stratigraphic interpretation and the definition of radarfacies were based on the method of seismostratigraphy adapted to GPR (Neal, 2004). The method is based on termination (onlap, downlap, toplap, and truncations), geometry, internal configuration, and pattern of reflections (Abreu et al., 2010; Leandro et al., 2019).

3.4. Modelling of barrier progradation

Finally, a simulation of coastal evolution was performed using the Geomorphic Model of Barrier, Estuarine and Shoreface Translations (GEOMBEST), which is a morphological-behaviour model that simulates the evolution of coastal morphology and the stratigraphy that results from changes in sea-level and sediment volume of a coastal barrier system. GEOMBEST was originally developed by Stolper et al. (2005) and later modified by Moore et al. (2010), Walters et al. (2014), Brenner et al. (2015) and Lauzon et al. (2018). The model considers conditions of mass (sediment) conservation during simulation of coastal evolution. The basic coastal variables necessary to run the model are: shoreface dimensions, dominant grain size, substrate slope and rate of sea-level fall over a specific time period. More details are available in Stolper et al. (2005). In this study, GEOMBEST was used to simulate the total progradation of YP at The Granites, in order to verify if the interpreted sea-level fall of 1.23 m was enough to produce the total observed progradation of 750 m.

Table 1
Radionuclides concentrations (^{238}U, ^{232}Th and K), dose rates (DR) and equivalent doses (ED) data used for calculation of OSL ages. N is the number of aliquots used for ED calculation and OD is the overdispersion of the ED distributions.

Sample	^{238}U (ppm)	^{232}Th (ppm)	K (%)	DR (Gy/ka)	N	ED(Gy) (CAM[a])	OD (%)	Ages (years)
Gran 2	0.67 ± 0.03	0.67 ± 0.05	0.061 ± 0.005	0.39 ± 0.02	22	1.7 ± 0.1	12.1	4367 ± 302
Gran 3	0.65 ± 0.03	0.67 ± 0.05	0.031 ± 0.003	0.41 ± 0.02	23	1.6 ± 0.0	8.3	3932 ± 252
Gran 4	0.65 ± 0.03	0.85 ± 0.06	0.140 ± 0.008	0.51 ± 0.03	24	2.1 ± 0.0	4.3	4133 ± 259
Gran 5	0.69 ± 0.03	0.88 ± 0.06	0.121 ± 0.007	0.51 ± 0.03	24	2.0 ± 0.0	10.6	3919 ± 258
Gran 6	0.67 ± 0.03	0.81 ± 0.06	0.137 ± 0.008	0.52 ± 0.03	24	2.1 ± 0.0	8.8	4055 ± 269
Gran 7	0.59 ± 0.03	0.67 ± 0.05	0.077 ± 0.005	0.44 ± 0.03	19	1.6 ± 0.1	16.3	3651 ± 265
Gran 8	0.62 ± 0.03	0.71 ± 0.05	0.170 ± 0.009	0.52 ± 0.03	23	1.8 ± 0.0	5.3	3447 ± 222
Gran 9	0.60 ± 0.03	0.72 ± 0.05	0.118 ± 0.007	0.48 ± 0.03	18	1.8 ± 0.0	7.8	3714 ± 244
Gran 10	0.53 ± 0.02	0.64 ± 0.05	0.067 ± 0.005	0.41 ± 0.03	24	1.5 ± 0.0	10	3646 ± 235
Gran 11	0.63 ± 0.03	0.78 ± 0.05	0.076 ± 0.005	0.46 ± 0.03	24	1.4 ± 0.0	9.9	3057 ± 203
Gran 12	0.63 ± 0.03	0.71 ± 0.05	0.106 ± 0.006	0.47 ± 0.03	23	0.2 ± 0.0	19.2	423 ± 34
Gran 2.1	0.75 ± 0.03	0.92 ± 0.06	0.096 ± 0.007	0.48 ± 0.03	22	1.7 ± 0.0	9.4	3517 ± 224
Gran 2.2	0.72 ± 0.03	1.06 ± 0.07	0.090 ± 0.007	0.42 ± 0.03	17	2.4 ± 0.1	7.8	5666 ± 448
Gran 7.5	0.81 ± 0.04	0.96 ± 0.07	0.178 ± 0.010	0.59 ± 0.04	24	1.8 ± 0.0	7.6	3053 ± 196
Gran 9.5	0.67 ± 0.03	0.79 ± 0.06	0.099 ± 0.007	0.48 ± 0.03	21	1.6 ± 0.1	16.1	3348 ± 295
Gran 11.5	0.69 ± 0.03	0.87 ± 0.06	0.096 ± 0.007	0.50 ± 0.03	17	0.8 ± 0.0	11	1588 ± 103
Gran 13	0.73 ± 0.03	0.92 ± 0.06	0.099 ± 0.007	0.51 ± 0.03	12	0.5 ± 0.0	22.6	988 ± 62

[a] CAM – Central Age Model.

Table 2
Radiocarbon AMS datings.

Sample	Beta analytic	Material dated	Depth range (m)	$\delta^{13}C$ (‰)	^{14}C a BP	^{14}C cal a BP[a]
Gran1-0	410905	Shell (*Anapella cycladea*)	1–30	+1.1	6020 ± 30	6990–6560
Gran1-29	411548	Shell (*Katelysia Scalarina*)	1–30	−1.8	6040 ± 30	6950–6525
Gran1-51-61	411549	Shell (*Anapela Cycladea*)	1–30	0.0	5910 ± 30	6840–6405
Gran1-75-77	411550	Shell (*Tatea Rufilabris*)	~1	+0.8	3210 ± 30	3580–3155

[a] Calibration to calendar years based on Reimer et al. (2013).

4. Results

4.1. Geomorphological analysis

The geomorphological analysis of the whole YP allowed the clear recognition of foredune ridges from Cape Jaffa up to 9 km to the north of The Granites (Figs. 2 and 4). At The Granites the YP barrier is 900 m wide and comprises at least 26 foredune ridges. Most of the barrier surface is positioned at 6–7 m above sea-level, but six ridges are considerable higher (Figs. 2 and 3). The innermost higher ridge started to form prior to around 5.6 ka and is 11 m high at the highest point. To the west (235 m seawards) a ridge formed at around 3.6 ka is 10 m high. 260 m further to the west there is a ridge which formed around 3.0 ka that is on average 10.5 m high. Finally the highest relict foredune-blowout ridge complex (formed comprising two ridges), that started to form close to 1.5 ka, has an average altitude of 14 m (Fig. 3). However, just adjacent to this portion of the ridge complex, the relict foredune rises to 22 m above AHD, so there is considerable variation in ridge height along this portion of the barrier. On average the ridge crest spacings are 30 m.

Towards the south, a few vegetated parabolic dunes occur, and the ridges are gently curvilinear alongshore, probably due to the action of wave refraction during barrier progradation promoted by the occurrence of shallow subsurface granite rocks (Fig. 1). Also, some ridges (e.g. the larger innermost one) split into two and then, four ridges (Fig. 4A and B) towards the south indicating a long-term southward increase in the rate of progradation, at least during the development of the inner portion of the barrier. Towards the north the barrier is slightly wider, and it starts to exhibit frequent modern blow outs and parabolic dunes, with the latter sometimes covering the whole barrier surface (Fig. 4C and D).

The bathymetric map of Fig. 5 shows isobaths fronting the Sir Richard and Younghusband Peninsula's across Encounter Bay. The orientation and greater distance of the 40, 30 and 20 m isobaths from the shoreline in The Granites coastal sector implies a substantial wave energy dispersion by wave refraction and wave attenuation by bottom friction, respectively; with a consequence of less wave energy in the surf zone, as previously attested by Short and Hesp (1984). The inner shelf slope is very gentle at The Granites (0.04° - measured from the shoreline to the 40 m isobath), whereas the central to northern portion of the shelf has a slope of 0.17°.

4.2. Geochronology and GPR

4.2.1. ^{14}C dating of lagoonal/estuarine sediments

At the back of the barrier, approximately 150 m to the east of the innermost dune ridge, a trench was excavated in the palaeo-lagoon and revealed a record of middle to late Holocene sedimentation of the lagoon/estuary. The four dates collected indicate that the lagoon/estuary was active between approximately 6.7 to 3.3 ka BP (Fig. 6, Table 2). The oldest record corresponds to a dark grey sand with in-life position, articulated shells of *Anapella cycladea*, collected at an altitude of 0.67 m above AHD, and dated at 6990–6560 cal yrs. BP. Above this is a contact with a sandy layer (0.56 m thick) with articulated shells of *Katelysia scalarina* at an altitude of 0.96 m and dated at 6950–6525 cal yrs. BP. In the middle of this sandy layer, at an altitude of 1.23 m, articulated shells of *Anapella cycladea* were dated at 6840–6405 cal yrs. BP. The top 10 cm of this sandy layer is pale brown (a pedogenic effect) and is marked by the presence (in high concentration) of the small gastropode *Tatea rufilabris*. Three well preserved shells of *Tatea* sp. were collected at an altitude of 1.43 m, and dated at 3580–3155 cal yrs. BP. This *Tatea* sp. layer is succeeded by 0.20 m of an incipient, weakly indurated weak calcrete, which is finally covered by 0.20 m of organic soil. See Table 2 for details of the ^{14}C dates.

According to Boyd (2017) and Boyd and Museums Victoria Staff (2017) both bivalves are modern species living in estuaries and in mud and sand flats, in waters depth varying from 0 to 30 m. The three similar ^{14}C dates (6990–6560, 6950–6525 and 6840–6405 cal yrs. BP) of *Anapella cycladea* and *Katelysea scalarina* correspond to sandy deposits formed under relatively protected marine conditions (lagoonal/estuary), and indicate the lagoon was open to the sea. Interpretation of a satellite imagery for the area indicates that there was very likely a lagoon entrance existent at the time at the southern end of the lagoon near Kingston SE. *Tatea rufilabris* (3580–3155 cal yrs. BP) is restricted

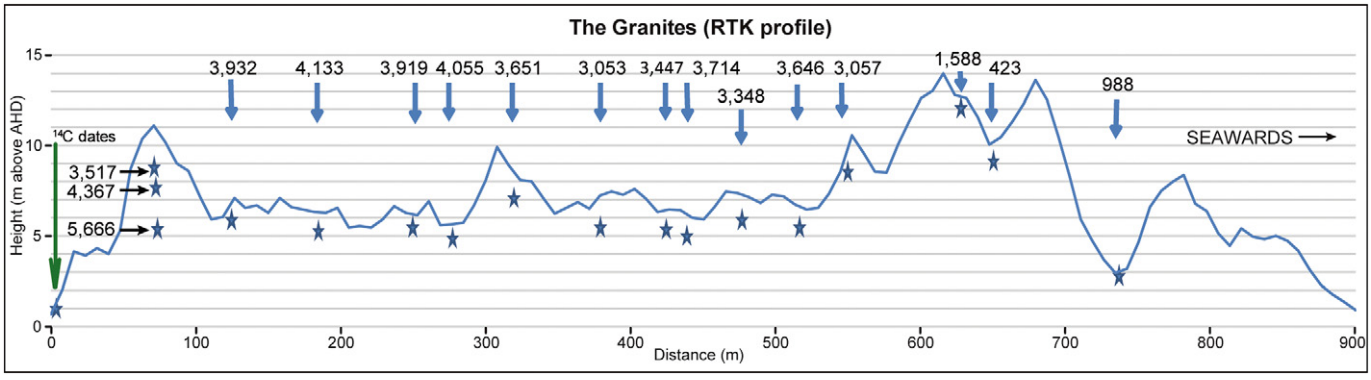

Fig. 3. RTK topographic profile of the barrier at The Granites (see profile location at Fig. 2), and location (stars) of OSL dates. See trench location at the lagoonal domain at the back of the barrier, where ^{14}C dates were obtained (see the extreme left of the figure indicated by the large arrow). Trench is presented in Fig. 6.

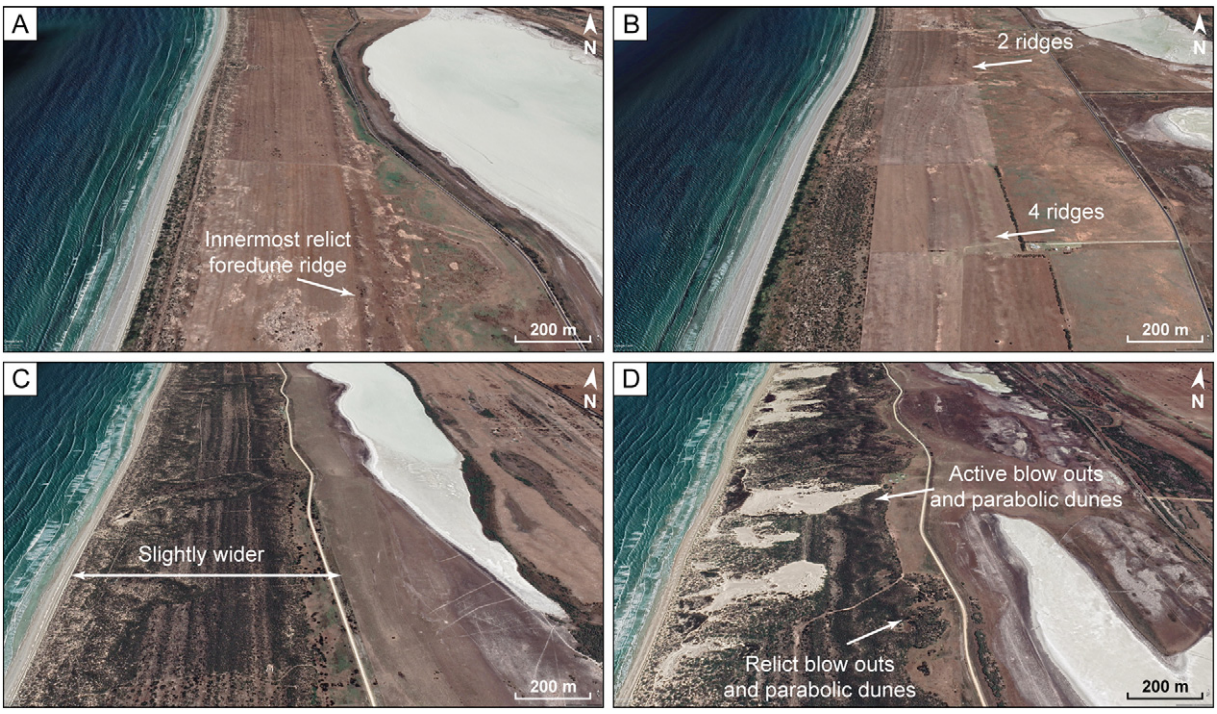

Fig. 4. Towards the south of The Granites, the innermost relict foredune ridge in (A) splits into 2 ridges and then further south into four ridges in (B). Towards the north the barrier is slightly wider (C) and relict and active blow outs and parabolic dunes are more frequent (D). See locations in Fig. 5.

to lagoons and estuaries, on the upper part of the shore. This species can tolerate a wide range of salinities including freshwater (Ponder et al., 1991), so the presence of this species likely indicates the lagoon was closed by this time.

The GPR record for this portion of the barrier-lagoon is presented in Fig. 7. The strata are clearly horizontal, long and laminar at the lagoonal domain (Fig. 7A).

4.2.2. OSL dates and GPR of the barrier relict foredune sediments

The barrier displays at least 26 foredune ridges across 900 m. Collection of samples for OSL dating was performed in 17 places across this relict foredune ridge system. The positions are shown in Fig. 3. All samples have quartz grains dominated by the fast OSL component, thus suitable for sediment dating (Murray and Wintle, 2003). Equivalent dose distributions have overdispersion ranging from 4.3 to 22.6%, indicating sediments completely bleached prior to deposition and without post-deposition mixing (Arnold and Roberts, 2009). Equivalent doses are in the range from 0.20 ± 0.05 Gy to 2.40 ± 0.01 Gy. Dose rates vary between 0.39 ± 0.02 Gy and 0.59 ± 0.04 Gy/ka, indicative of very homogeneous sediments rich in quartz. Details of the dates are presented in Table 1.

In general, the results indicate that the larger, innermost ridge was formed at least from 5.6 to 4.3 ka. Taking into account the other ages of barrier progradation, the age of 3.5 ka close to the top of the ridge might represent a later phase of reworking, in a time when the barrier had already prograded approximately 250 m. The relatively high angle strata on the seaward margin of the ridge (indicated in Fig. 7B) may be a scarp further suggesting that the ridge was partially destabilized approximately post-3500 years ago. The GPR record of this innermost part of the barrier has reflectors (arrowed in Fig. 7B) which are palaeosols and bounding surfaces separating three phases of aeolian activity that formed this inner ridge (Figs. 7B and 8).

The older age (phase) of 5.6 ka is the minimum age of formation of the ridge since we only obtained this date by drilling 1 m into the ridge below the road cutting surface (see auger at the bottom of the ridge in Fig. 8A). That is, we quite likely did not intercept the deepest oldest aeolian sediments. Later, phases 2 and 3 dated at approximately 4.3 and 3.5 ka finalized the construction of the first ridge. From 5.6 ka to at least 4.3 ka the barrier behaved as an aggradational (stationary) barrier. The late phase dated to 3.5 ka was formed when the barrier had already prograded up to the middle ridge, which was dated at 3.6 ka.

Following this aggradational phase, there was a phase of progradation where approximately 20 ridges were formed in 1300 years (Fig. 3). Most of the barrier progradation developed from 4.3 to 3.0 ka, over a distance of 500 m and under a generally low rate of progradation of 0.38 m/yr. The last dated phase of barrier progradation was contemporaneous with a significant aggradational phase, and occurred from post-3.0 to 1.0 ka (the 1.0 ka age is in fact an OSL age of 988 yrs.), over a distance of 190 m, corresponding to a very low rate of progradation of 0.09 m/yr. A small modern foredune is present on the seaward margin and likely developed here post-1978 when *Thinopyrum junceiforme* (Seawheat grass) began to invade the region and formed extensive incipient foredunes (Hilton et al., 2006).

Fig. 9 shows the GPR record of a 70 m long section that illustrates a portion of the main phase of progradational behavior of the barrier. Due to the quality of the GPR data, only a short section is presented.

The backshore-foreshore radarfacies (Rdf2) shows GPR reflectors which are continuous, sub-parallel and dipping seawards at a low angle in similarity to the modern low angle beach. The aeolian (foredune) radarfacies (Rdf1) has GPR reflectors that are non-continuous, undulating, relatively short and at moderate angles (foredune ridges). The ridges display classic stratification associated with aeolian deposition within plants on the backshore, followed by gradual buildup and seawards progradation as shown in foredune formation and stratification studies by, for example, Hesp (1983, 1988b, 1989), McLean and Shen (2006), Hesp (2013), Barboza et al. (2013), and Costas et al. (2016).

The OSL samples have relatively homogenous compositions regarding radionuclides concentrations and equivalent dose distributions with low overdispersion (<23%) pointing to well-bleached sediments without post-depositional mixing. Therefore, the apparent inversion of some ages across the barrier (see Fig. 3) might be attributed to age

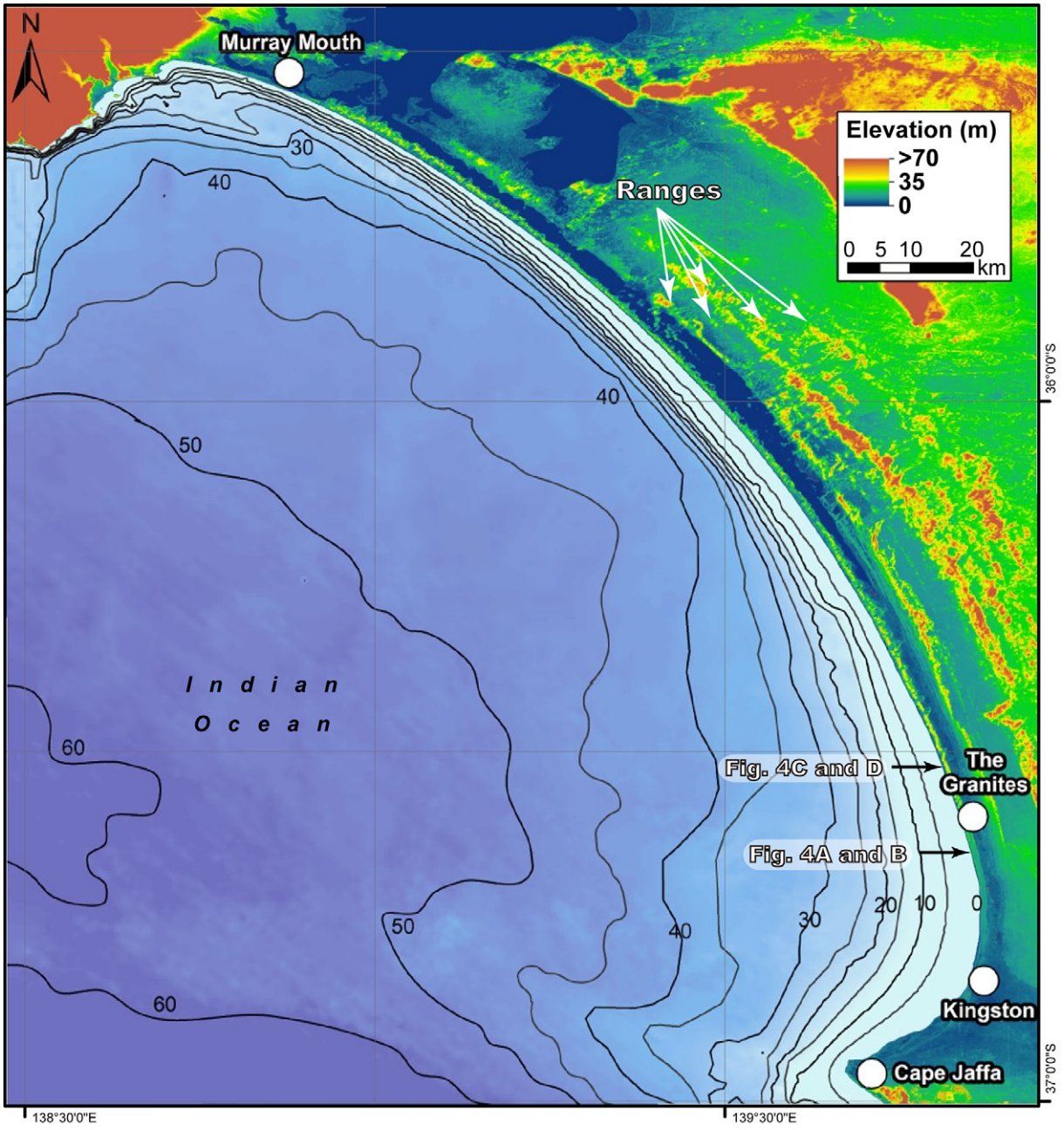

Fig. 5. Bathymetric map of Encounter Bay showing isobaths from 5 to 60 m. The landwards yellow and orange strips are Pleistocene coastal barriers (Ranges of Fig. 1). (Source: bathymetry from GEBCO - 2019, and Digital Surface Model (DSM) of ALOS World 3d.

variation due to different sampling depth, influence of water content on dose rate, post-ridge formation sedimentation due to a major wind event, or blow-outs starting in a more seawards ridge and developing over older landward (relict) ridges. The latter was indicated by Oliver et al. (2014) at Moruya (New South Wales). Fig. 9, for example, clearly shows sedimentation within and partial burial of a swale post-ridge formation. Since we obtained quite shallow samples for dating, it is quite possible that we intersected and dated younger sediments located in a landwards position of older sediments. Variation of water content through time can also play some role for OSL ages inconsistencies. The falling of water table and progradation can reduce the water content of sediment deposited underwater like wave-deposits. Then, the reduced water content recorded during sampling would not represent the water content since sediment deposition, promoting dose rate overestimation and, consequently, age underestimation.

Several topographic surveys indicated that the limit between the active foredune and modern backshore/foreshore deposits (or the active foredune-beach contact) is at 3.0 m above AHD. Observing that this contact in relict foredune-beach deposits of GPR section of Fig. 9 is occurring at 4.5 to 4.0 m above AHD, and assuming the same gradient for modern and palaeo-beach, it might be argued that at this phase of barrier progradation sea-level was positioned at approximately +1.5 to +1.0 m.

5. Discussion

5.1. Sea-level height during the middle and late Holocene

The integration of ^{14}C dates of lagoonal/sheltered marine molluscs (*Anapella cycladea* and *Katelysea scalarina*) and OSL dates of the high innermost ridge indicates that: i) at around 6.7 ka BP the Coorong lagoon was experiencing a significant influence of marine waters, providing

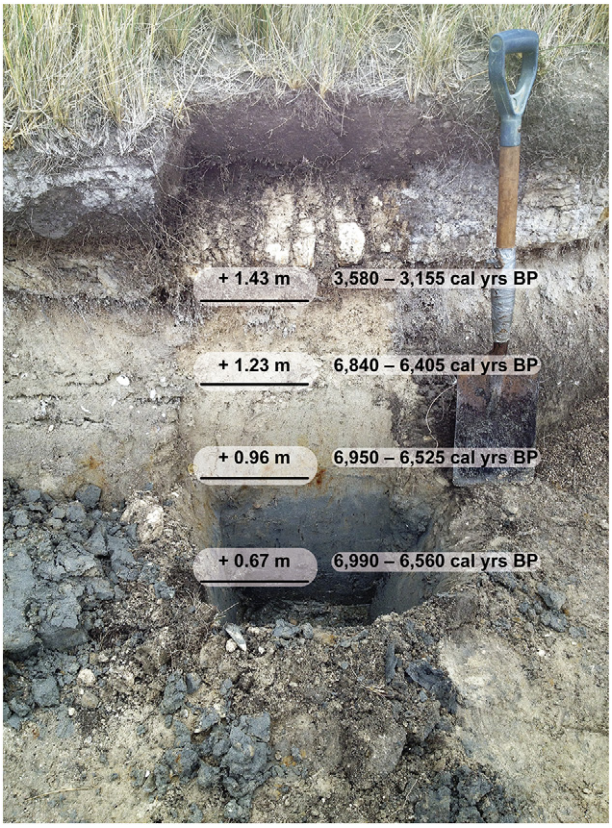

Fig. 6. Trench excavated in the palaeo-lagoon landwards of The Granites barrier. The heights above AHD and ^{14}C dates are indicated. See trench location in Figs. 2 and 3.

adequate environmental conditions for *Anapella* and *Katelysea* colonisation. Therefore, a southern inlet of the lagoon was very likely open and active at that time; and ii) from 6.7 ka BP to 4.3 ka the barrier system behaved as a stationary/aggradational barrier. The presence of marine waters in the lagoon at the initial phases of barrier formation could be an indication that sustains the interpretation of Harvey et al. (2006) and Bourman et al. (2016) that the barrier was initially formed as several segmented barrier islands, or perhaps as a single island extending from the Murray mouth to Kingston (SE). Either situation, with the presence of a single inlet at the southern sector of the YP would produce the same result.

Considering that the lagoonal/estuary or shallow marine molluscs (*Anapella cycladea* and *Katelysea scalarina)* found in the palaeo-lagoon immediately adjacent to the back of The Granites barrier were found in life position, and in heights varying from +0.67 to +1.23 m (this height being the top of the estuarine record), it is suggested that the altitude of sea-level in the middle Holocene (around 6.7 ka BP) was positioned at least around +1.23 m at The Granites. The gastropode *Tatea rufilabris* was found at 1.43 m above AHD, and due to the fact this gastropod can tolerate a wide range of salinities including freshwater (Ponder et al., 1991), sea level was likely to be lower than this, and the lagoon closed at the southern end by approximately 3.3 ka BP or earlier. This value of +1.23 m is very close to the maximum sea-level of 1 m reached during the Holocene as shown for Port Lincoln (415 km distant from The Granites) by Belperio et al. (2002).

As mentioned above, the contact of the active (modern) foredune toe and the top of the backshore at The Granites beach region is located at an altitude averaging 3.0 m. The relict contact marked in Fig. 9 (small black arrows) is positioned at altitudes varying from 4.5 m to 4.0 m, at a time close to 3.9 ka. This relict contact between foredune and backshore deposits, commonly found in progradational coastal barriers is a frequently used sea-level indicator (Tamura, 2012; Costas et al., 2016; Oliver et al., 2019b). By simply subtracting the altitude of the modern

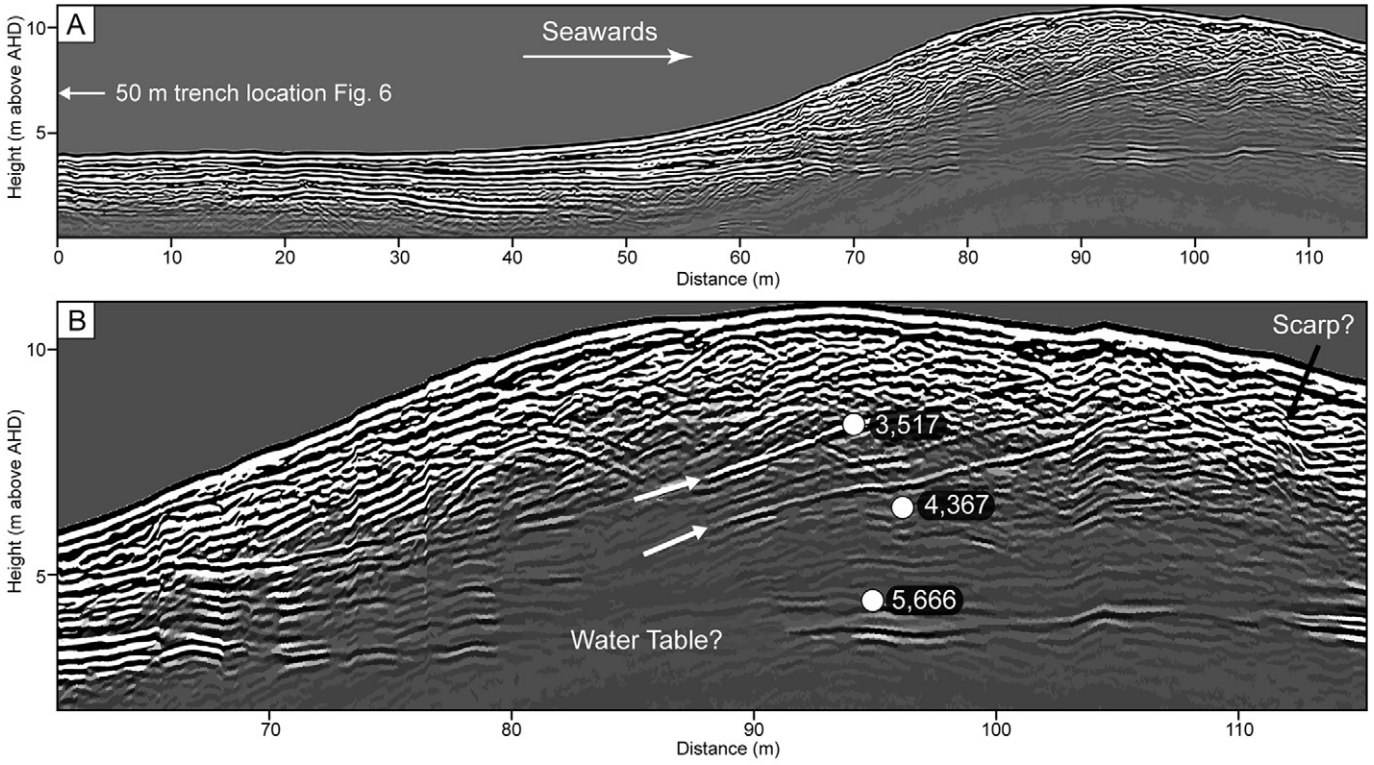

Fig. 7. (A) General GPR record of the oldest first relict foredune of The Granites barrier (GX 160 MHz antenna). The horizontal backbarrier/lagoon sediments are on the left, and trench of Fig. 6 is 50 m to the left of the GPR record. (B) Detail of the ridge strata showing two clear bounding surfaces (marked by white arrows) both of which are proven palaeosols, and OSL ages of samples Gran 2.2, Gran 2 and Gran 2.1 (from base to top). Fig. 2 shows location of GPR profile.

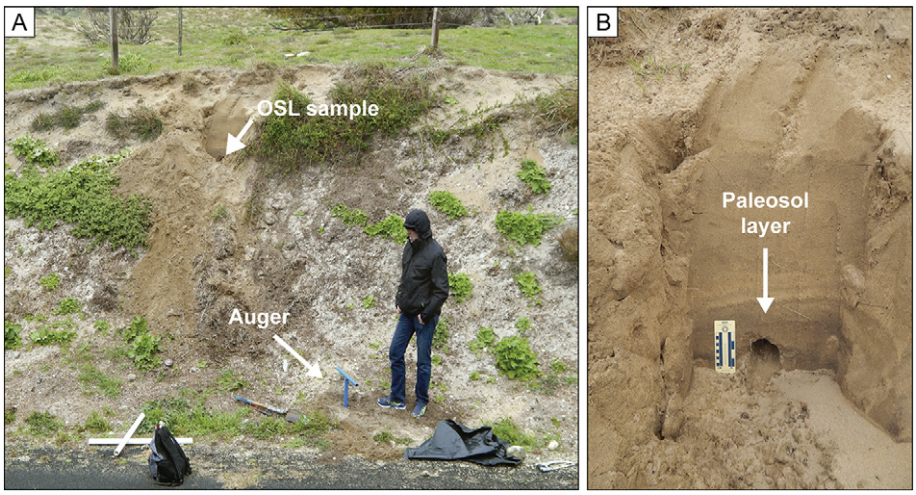

Fig. 8. (A) View of the road cutting through the oldest foredune ridge on the landward margin of the barrier and location of photograph B (white arrow). (B) Weakly developed palaeosol and OSL sampling hole near the crest of the oldest foredune ridge at The Granites. The palaeosol shown in B dated at 3517 yrs.

contact of this relict contact, it might be stated that at around 3.9 ka, during the main phase of barrier progradation sea-level was positioned at around +1.5 to +1.0 m. These altitudes are very coherent with the ones obtained by the paleontological records of the lagoonal sediments, which have indicated a sea-level of around +1.23 m at around 6.7 ka BP, and together these altitudes indicate an insignificant sea-level oscillation from 6.7 ka BP to 3.9 ka. Also, these heights of paleo sea-level of +1.5 to +1.0 m, interpreted from the GPR record of Fig. 9, are slightly lower than the heights of +2.3 to +1.7 m that have occurred at around 3.5 ka in Rivoli Bay according to Oliver et al. (2019b). Rivoli bay is 100 km distant (in a straight line) southwards of The Granites. It is important to mention here that as stated by Oliver et al. (2019b) these height values contain uncertainties due to antenna resolution of the GPR system, topographic correction and natural variability of the beach/dune contact.

5.2. Barrier evolution and nearshore-shelf bathymetry

The barrier morphology in The Granites region clearly indicates the largely regressive (or progradational) nature of the whole barrier along this coastal sector. Prograded foredune ridges dominate the barrier from Cape Jaffa up to 9 km north of The Granites, a distance of approximately 40 km. An analysis of the bathymetric map of the entire embayment (Fig. 5) indicates that there may exist a close relationship

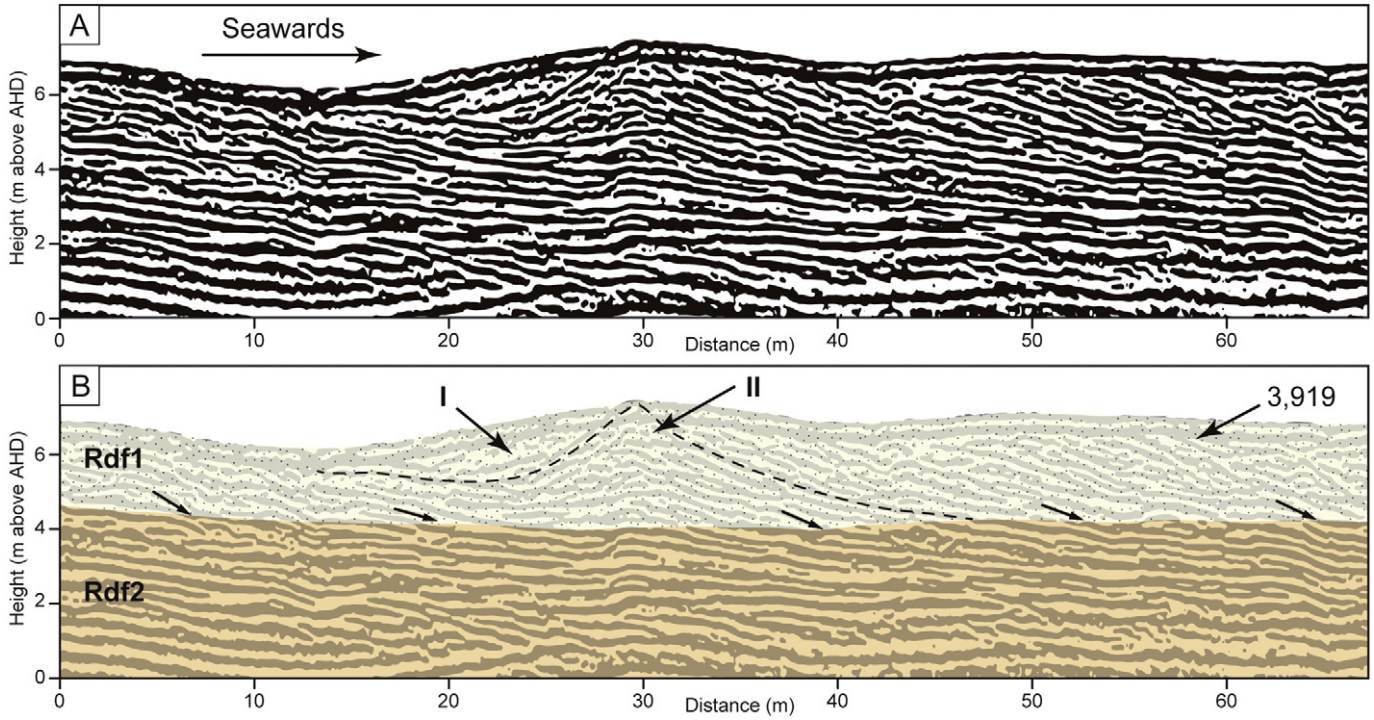

Fig. 9. GPR record (antenna GX 450 MHz) of a 70 m long section in the early portion of the progradational phase (start location 80 m seawards of the toe of the first most landward ridge) illustrating the typical stratigraphic pattern of prograding foredune ridges (Rdf1 and II) and backshore-foreshore facies (Rdf2), with an infilled swale leeward (I) or landwards of the ridge crest. 3919 is an OSL age (yrs). The strata display classic aeolian sedimentation in plants above a prograding backshore. A date in the infilling sediments (I) would very likely produce a date younger than a date collected below the seawards ridge crest. The small black arrows indicate the interpreted position of the limit between relict foredune-beach deposits. Fig. 2 shows location of GPR profile.

between shelf slope and the northern limit of barrier progradation. Note that we currently do not know if the transgressive dunefield to the north also prograded during its evolution, either in part, or fully. Approximately at the northern limit of visible relict foredune ridges (9 km to the north of The Granites), the adjacent inner shelf shows an abrupt change of isobath orientation, with the 50, 40 and 30 m isobaths turning to the east, and trending to approach the coastline (Fig. 5). This abrupt change of isobaths orientation indicates that, from this point towards the north, wave energy increases due to a presence of a steeper shelf slope producing less wave energy dissipation by bottom friction. Average slope changes from 0.04° at The Granites to an average 0.17° at the central-north sector of Encounter Bay. Differences in the order of 0.1° degrees of shelf slope produces significant changes on wave energy dissipation by bottom friction (Wright, 1976; Schwab et al., 2000; Dillenburg et al., 2000). In addition, the isobath configuration from this point southwards towards Kingston-Cape Jaffa favors wave energy dissipation by refraction also. The point here is that barrier progradation via foredune ridge development is likely an effect driven by low wave energy that favored conditions for coastal stability and foredune formation. In contrast, the dunefields to the north are transgressive dunefields formed in a higher wave energy environment where shoreline stability was significantly less.

As noted above, a geomorphological analysis of the barrier towards the north shows that the most landwards high relict foredune ridge continues to around 9 km towards the north. However, as one trends 5.2 km to the south of the Granites, the innermost ridge initially splits into two and then eventually four ridges (Fig. 4A, B). Thus, the inner part of the barrier trends from aggradational/progradational at The Granites and few kilometers to the north, to progradational towards the south. This indicates an increased rate in barrier progradation towards the south during the initial phase of barrier evolution.

5.3. Barrier progradation and Aeolian reworking phases

The regressive phase of the barrier, as previously noted occurred initially at an average rate of progradation of 0.38 m/yr (from 4.3 to 3.0 ka), followed by a significant decrease from 3.0 to 1.0 ka, when the barrier prograded at a very low rate of 0.09 m/yr. Carvalho et al. (2019) in a comparison of rates of progradation between barriers developed in similar coastal environments of east, southeast and south Australia found rates varying from 0.1 to 0.39 m/yr. Despite being a distinct coastal site (ocean open), the southern sector of the YP is relatively protected from very high energy waves, showing an autogenic source of sediments (marine source), with similarly low rates of progradation.

Starting from the innermost 11 m high ridge, an additional 25 ridges were formed in a time interval of approximately 4.3 ka, resulting in a total barrier progradation of 750 m. The Murray River, Currency Creek and Finniss River built deltas inside lakes Alexandrina and Albert and did not therefore supply sediments for barrier construction at the coast. As a consequence, riverine sediments have not been delivered to the coast in the last millenia (at least since 7–6 ka when the Holocene barrier was formed) (Bourman et al., 2016). Thus, it can be argued that the evolution and growth of the YP Holocene barrier was possible by the cross-shore, and possibly alongshore sand transference of nearshore and shelf sediment onto the beach-shoreface system as occurred for many coastal barriers in Eastern and SE Australia (Thom and Roy, 1985; Thom et al., 1992; Oliver and Woodroffe, 2016; Oliver et al., 2017, 2019a). Therefore, progradation of the barrier at The Granites was possible due to one or possibly both of the above-mentioned processes of wave driven onshore sand transport.

The analysis of both the distribution of OSL dates on the foredune ridge plain and of the GPR record of Fig. 9 warrants further examination of the five age inversion pairs depicted in Fig. 3. Starting at the innermost and oldest ridge the pairs start with 3932/4133 and follow with 3919/4055; 3053/3447; 3447/3714 and 3348/3646 ka. As the first age of each pair may represent the age record of a major wind event, or blow-out initiation we might argue that one or both processes were active at around 3.9 ka (two ages); 3.5 to 3.3 ka (including the last phase of construction of the innermost ridge which is 3.5 ka, totaling three ages varying from 3.3 to 3.5 ka); and finally the age of 3.0 ka which is the same age of one of the highest ridges located 245 m landwards from the present shoreline. In summary, these OSL date inversions could be the result of the reworking of ridges by subsequent wind/blow-out events occurring approximately at around 3.9, 3.4 and 3.0 ka. These ages suggest the occurrence of aeolian action each operating over 500 to 400 yrs. Recent research by Goodwin et al. (2006, 2014) along the Australian east coast indicates that major shifts in the modal climate operated at millennial to centennial time scales, at least since 3.0 ka, with a most recent shift occurring post-1600 to 1800 CE driving considerable changes in storm frequency, wave driven sediment transport, and foredune transgression. Perhaps such changes in the modal wave climate occurred previously in the 4.3 to 3.0 ka period also driving significant aeolian reworking of barrier surfaces and ridges.

Future research on prograded barriers of Australia and even on barriers of the southern hemisphere should pursue the potential existence of teleconnected records of coastal events such as storms and aeolian activity.

5.4. Holocene Tectonics and source of sediments for barrier progradation

Encounter Bay has a variable tectonic gradient alongshore. According to Bourmann et al. (2016) The Granites region is rising at a rate of 0.07 mm/yr, while the Murray River mouth is sinking at a rate of 0.02 mm/yr. This tectonic activity has very likely occurred throughout the Holocene. As the YP barrier started to form at around 7.0 ka BP, the NW block of Encounter Bay may have downfaulted approximately 14 cm since that time, and the SE block risen approximately 49 cm. Considering this variable (a local relative sea-level) as the only one affecting coastal evolution, the NW block evolved under a relative sea-level rise at a rate of 0.02 mm/yr, while at the same time the SE block was subjected to a relative sea-level fall at a rate of 0.07 mm/yr. Are such rates of sea-level rise and fall significant for barrier evolution during the middle and late Holocene? This discussion will be limited to The Granites region only, and the highest sea-level of +1.23 m, indicated by the paleontological record of sea-level position at around 6.7 ka BP will be considered. Since barrier progradation took place in a period of 4.3 ka, the potential amount of tectonic sea-level fall for The Granites was 31 cm during the progradation period. In a very simple approach, it must be considered that this 31 cm is included in the total of 1.23 m of relative sea-level fall interpreted in this present study for The Granites region in the last 4.3 ka, based on the above mentioned records of lagoonal sedimentation. Few studies have been conducted of the sea level histories of open ocean barriers in South Australia. According to Belperio et al. (2002) sea-level probably reached approximately 1 m above present sea-level at around 7 ka on open ocean beaches (i.e. not up the Gulfs). If 0.49 m is subtracted (local tectonic cause of sea-level fall since 7.0 ka BP) from 1.23 m (paleontological record of sea-level position at 6.7 ka BP, roughly 7.0 ka BP), we derive +0.74 m as a sea-level position above the present level, produced by allogenic (external) factors controlling sea-level in South Australia during the middle and late Holocene.

However, the important question here is: was the total sea-level fall of 1.23 m the main factor that produced a progradation of 750 m at The Granites? To answer this question a modelling exercise using GEOMBEST was performed. The basic coastal variables used in the simulation were: shoreface dimensions (X = 3000 m and Y = 15 m), dominant grain size: fine sand, substrate slope: 0.025°and rate of sea-level fall over a total time of 4.3 ka. The modelling results indicate that the sea-level fall of 1.25 m (this value was used to simplify the modelling, instead of 1.23 m) extending from the shoreface toe to the open sea would have produced progradation at The Granites varying from 769 to 1137 m (Table 3). This modelling result indicates that the forced

regression produced by a sea-level fall of 1.23 m would be enough to produce sediments necessary for a progradation of 750 m as observed at The Granites. This process of progradation, where sea-level fall triggers the process of onshore sand transport to produce barrier progradation is well presented by Roy et al. (1994, see their Fig. 4.11).

A similar simulation of coastal evolution was performed on the barrier coast of southern Brazil by Dillenburg et al. (2000), using the Shoreface Translation-Barrier Model (STM) (Cowell et al., 1991). The provenance of sand for the observed progradation at The Granites could include the process of sand transference from the shoreface driven by disequilibrium morphology (Kinsela et al., 2016), which basically considers that when the maximum sea-level of the Post-Glacial Marine Transgression (PMT) was established, the shoreface morphology was not equilibrated with the new dynamic conditions. To establish equilibrium, a natural readjustment of the shoreface surface was necessary, which in turn implied erosion and the transport of sand to the beach (cf. Roy and Thom, 1981; Thom et al., 1981). In conclusion, no external source of sand was necessary for the progradation of the Holocene barrier of the YP along The Granites coastal stretch in the last 4.3 ka.

5.5. Large foredune ridge formation in the last 3 ka

From 3.0 ka (3057 yrs) to 1.0 ka (988 yrs), the barrier prograded over a distance of only 190 m, corresponding to an average rate of 0.09 m/yr). Over this short distance of progradation four ridges were formed with mean heights varying from 10.5 to 13.5 m (Fig. 3). However, just adjacent and southwards of this portion of the ridge complex, the highest relict foredune shown in Fig. 3 rises to 22 m above AHD, so there is considerable variation in ridge height along this portion of the barrier. The heights here are almost the double those of the innermost and middle ridge. The age of 423 years obtained for a shallow sample collected in the swale between the most developed ridges (see Fig. 3), probably indicates the occurrence of a recent wind/blow-out event, similar to the ones interpreted to have occurred in a multi-centennial scale (500–400 yrs) during the main phase of barrier progradation (4.3 to 3.0 ka).

Two hypotheses, not excluding each other were recently presented to explain such large foredune formation close to the shoreline in southeast Australia. Following previous work by Davies (1957), Shepherd (1987), Hesp (2002) and Davidson-Arnott et al. (2018), Oliver et al. (2019a) suggested that the height of a ridge is the result of the rate of shoreline progradation, whereby rapid and slower progradation produces low and higher ridges, respectively. This hypothesis is consistent with the decrease of progradation rate at The Granites from 0.38 to 0.09 m/yr at around 3.0 ka. An alternative hypothesis is that the longer a foredune ridge remains active at the rear of the beach, the larger the ridge on average, since the sequence of storm wave scarping, scarp fill, aeolian sand delivery up the scarp fill, crestal deposition and foredune growth and potentially translation leads to larger more complex foredunes over time (Hesp, 1988b; Davidson-Arnott et al., 2018). A large complex foredune development post-500 yrs ago is also consistent with Goodwin et al. (2006, 2014) indication of greater storminess and foredune scarping and transgression as noted above.

Table 3
Simulation with GEOMBEST of the total progradation at The Granites under different RSL fall and extension of erodible substrate.

Case	RSL[a] fall (m)	Substrate slope	Erodible substrate – shoreface toe to open sea (m)	Progradation (m)
1	1.25	0.025°	No limit	1137
2	1.25	0.025°	7200	894
3	1.25	0.025°	5000	871
4	1.25	0.025°	3000	769

[a] RSL – relative sea-level.

6. Conclusions

The initial development of The Granites barrier system began as an aggradational barrier comprising a single foredune which underwent at least two phases of stabilization and reactivation/further building from 6.7 ka BP to 5.6 ka to 4.3 ka. The lagoon experienced full tidal exchange at a sea level higher than present. Barrier progradation of 750 m at The Granites started at around 4.3 ka and developed a suite of foredune ridges at a progradation rate of 0.38 m/yr. In the latter stages of barrier development, the rate of progradation slowed considerably to 0.09 m/yr and may have experienced landwards translation and aggradation rather than progradation given the quite large foredune complexes formed at this time (last 1.5 ka). During the development of the barrier in a time period from 6.7 ka BP to 3.9 ka paleontological data from lagoonal sediments and GPR data from the foredune plain indicate that sea-level stayed positioned at around +1.23 and + 1.5 m, respectively.

During the main phase of barrier progradation which occurred from 4.3 to 3.0 ka at least three phases of significant aeolian activity reworked the barrier surface, promoting the increased deposition on some ridges and the infilling of landward swales that (possibly) caused an apparent inversion of some OSL ages. These three phases were active at around 3.9, 3.4 and 3.0 ka, suggesting the occurrence of aeolian action at 500 to 400 years intervals. This centennial scale of aeolian disruption deserves future investigation of potential teleconnections with aeolian activity elsewhere, at a regional and even continental scale. The progradational behavior of this southern sector of the YP (around 40 km in lenght) seems to be an effect driven by a low wave energy, established by a gentle shelf slope that favored conditions for coastal stability and foredune formation.

Computer modelling indicates that the forced regression produced by a relative sea-level fall of 1.23 m only would be enough to produce the amount of sediments necessary to the observed progradation of the barrier.

Declaration of competing interest

The authors declare that they have no known competing financial interests or personal relationships that could have appeared to influence the work reported in this paper.

Acknowledgements

We thank CAPES/Brasil funding to S. Dillenburg for a visiting sabbatical Fellowship at Flinders University (grant no BEX 5287/14-6) and Flinders University College of Science and Engineering for support. S. Dillenburg, E. Barboza and A. Sawakuchi also thank CNPq/Brasil for the provision of their research fellowships. P. Hesp. G. Miot da Silva, I. Moffat and R. Keane thank the BEADS Lab and Flinders University College of Science and Engineering for support.

References

Abreu, V.S., Neal, J., Vail, P.R., 2010. Integration of sequence stratigraphy concepts. In: Abreu, V.S., Neal, J., Bohacs, K.M., Kalbas, J.L. (Eds.), Sequence Stratigraphy of siliciclastic systems – The ExxonMobil Methodology: atlas of exercises. Concepts in Sedimentology and Paleontology 9, 2nd edition, SEPM, pp. 209–224.

Aitken, M.J., 1998. An Introduction to Optical Dating. Oxford University Press, New York (280p).

Arnold, L.J., Roberts, R.G., 2009. Stochastic modeling of multi-grain equivalent dose (De) distributions: implications for OSL dating of sediment mixtures. Quat. Geochronol. 4, 204–230. https://doi.org/10.1016/j.quageo.2008.12.001.

Banerjee, D., Hildebrand, A.N., Murray-Wallace, C.V., Bourman, R.P., Brooke, B.P., Blair, M., 2003. New quartz SAR-OSL ages from the stranded beach dune sequence in southeast South Australia. Quatern. Science Rev. 22, 1019–1025. https://doi.org/10.1016/S0277-3791(03)00013-1.

Barboza, E.G., Rosa, M.L.C.C., Dillenburg, S.R., Tomazelli, L.J., 2013. Preservation potential of foredunes in the stratigraphic record. J. Coast. Res. SI 65, 1265–1270. https://doi.org/10.2112/SI65-214.1.

Belperio, A.P., Harvey, N., Bourman, R.P., 2002. Spatial and temporal variability in the Holocene palaeosea-level record around the South Australian coastline. Sedim. Geol. 150, 153–169. https://doi.org/10.1016/02688699646961.
Bourman, R.P., Murray-Wallace, C.V., 1991. Holocene evolution of a sand spit at the mouth of a large river system: Sir Richard Peninsula and the Murray Mouth, South Australia. Zeitschrift für Geomorphologie. Suppl.-Bd. 81, 63–83.
Bourman, R.P., Murray-Wallace, C.V., Belperio, A.P., Harvey, N., 2000. Rapid coastal geomorphic change in the River Murray Estuary of Australia. Mar. Geol. 170, 141–168. https://doi.org/10.1016/S0025-3227(00)00071-2.
Bourman, R.P., Murray-Wallace, C.V., Harvey, N., 2016. Coastal Landscapes of South Australia. University of Adelaide Press (405 p).
Bourman, R.P., Murray-Wallace, C.V., Ryan, D.D., Belperio, A.P., 2018. The geological evolution of the River Murray Estuary Region. In: Mosley, L., Ye, Q., Shepherd, S., Hemming, S., Fitzpatrick, R. (Eds.), The Natural History of the Coorong, Lower Lakes and Murray Mouth Region (Yarluwar-Ruwe). Royal Society of South Australia, pp. 37–69. https://doi.org/10.20851/natural-history-cllmm-2.1.
Boyd, S., 2017. *Anapella cycladea* Bivalve Mollusc in Museums Victoria Collections. https://collections.museumvictoria.com.au/species/14320.
Boyd, S., Museums Victoria Staff, 2017. *Katelysea scalarina* Stepped Venerid in Museums Victoria Collections. https://collections.museumvictoria.com.au/species/8635, Accessed date: 11 September 2019.
Brenner, O.T., Moore, L.J., Murray, A.B., 2015. The complex influences of back-barrier deposition, substrate slope and underlying stratigraphy in barrier island response to sea-level rise: insights from the Virginia Barrier Islands, Mid-Atlantic Bight, U.S.A. Geomorphology 246, 334–350. https://doi.org/10.1016/j.geomorph.2015.06.014.
Carvalho, R.C., Oliver, T.S.N., Woodroffe, C.D., 2019. Transition from marine to fluvial-dominated sediment supply at Shoalhaven prograded barrier, southeastern Australia. Geomorphology 341, 65–78. https://doi.org/10.1016/j.geomorph.2019.05.010.
Cook, P.J., Colwell, J.B., Firman, J.B., Lindsay, J.M., Schwebel, D.A., von der Borch, C.C., 1977. The late Cainozoic sequence of southeast South Australia and Pleistocene sea-level changes. BMR J. Australian Geol. and Geophys. 2, 81–88.
Costas, S., Ferreira, Ó., Plomaritis, T.A., Leorri, E., 2016. Coastal barrier stratigraphy for Holocene high-resolution sea-level reconstruction. Sci. Rep. 6, 38726. https://doi.org/10.1038/srep38726.
Cowell, P.J., Roy, P.S., Jones, R.A., 1991. Shoreface translation model: application to management of coastal erosion. In: Brierley, G., Chappell, J. (Eds.), Applied Quaternary Studies. Canberra, Department of Biogeography and Geomorphology, A.N.U, pp. 57–73.
Curray J.R., Emmel, R.J., Crampton, P.J.S., 1969. Holocene history of a strandplain lagoonal coast, Nayarit, Mexico. In: Castanares, A.A., Phleger, F.B. (Eds.), Coastal Lagoons, A Symp. Univ. Nacional Autónoma de Mexico, Ciudad Univ., pp. 63–100.
Davidson-Arnott, R., Hesp, P.A., Ollerhead, J., Walker, I., Bauer, B., Delgado-Fernandez, I., Smyth, T.A.G., 2018. Sediment budget controls on foredune height: a comparison of cimulation model results and field data. Earth Surf. Process. Landforms 43, 1798–1810. https://doi.org/10.1002/esp.4354.
Davies, J.L., 1957. The importance of cut and fill in the development of sand beach ridges. The Australian J. Science 20, 105–111.
Davis, J.L., Annan, A.P., 1989. Ground-penetrating radar for high-resolution mapping of soil and rock stratigraphy. Geophys. Prospect. 37, 531–551. https://doi.org/10.1111/j.1365-2478.1989.tb02221.x.
Department for Energy and Mining, the Government of South Australia, Best practice regulation, sourced on 16 September 2019, https://data.sarig.sa.gov.au/downloads/mapsheets/250k/SJ5402.pdf, SJ5406, SJ5413, SJ5414.
Dillenburg, S.R, Hesp, P.A., 2009. Coastal barriers – an introduction. In: Dillenburg, S.R., Hesp P.A. (Eds.), Geology and Geomorphology of Holocene Coastal Barriers of Brazil. Springer, Lecture Notes in Earth Sciences 107, pp. 1–15. doi:https://doi.org/10.1007/978-3-540-44771-9_1.
Dillenburg, S.R., Roy, P.S., Cowell, P.J., Tomazelli, L.J., 2000. Influence of antecedent topography on coastal evolution as tested by the Shoreface Translation-Barrier Model (STM). J. Coast. Res. 16, 71–81.
Dillenburg, S.R., Tomazelli, L.J., Hesp, P.A., Barboza, E.G., Clerot, L.C.P., Silva, D.B., 2006. Stratigraphy and evolution of a prograded, transgressive dunefield barrier in southern Brazil. J. Coast. Res. SI 39, 132–135.
Dillenburg, S.R., Barboza, E.G., Tomazelli, L.J., Hesp, P.A., Clerot, L.C.P., Ayup-Zouain, R.N., 2009. The Holocene Coastal Barriers of Rio Grande do Sul. In: Dillenburg, S.R., Hesp P.A. (Eds.), Geology and Geomorphology of Holocene Coastal Barriers of Brazil. Springer. Lect. Notes Earth Sci. 107, 53–91. https://doi.org/10.1007/978-3-540-44771-9_3.
Dillenburg, S.R., Barboza, E.G., Rosa, M.L.C.C., Caron, F., Sawakuchi, A.O., 2017. The complex prograded Cassino barrier in Southern Brazil: Geological and morphological evolution and records of climatic, oceanographic and sea-level changes in the last 7-6 ka. Mar. Geol. 390, 106–119. https://doi.org/10.1016/j.margeo.2017.06.007.
Galbraith, R.F., Roberts, R.G., Laslett, G.M., Yoshida, H., Olley, J.M., 1999. Optical dating of single and multiple grains of quartz from jinmium rock shelter, northern Australia, part 1, experimental design and statistical models. Archaeometry 41, 339–364. https://doi.org/10.1111/j.1475-4754.1999.tb00987.x.
Goodwin, I.D., Stables, M.A., Olley, J.M., 2006. Wave climate, sand budget and shoreline alignment evolution of the Iluka–Woody Bay sand barrier, northern New South Wales, Australia, since 3000 yr BP. Mar. Geol. 226, 127–144. https://doi.org/10.1016/j.margeo.2005.09.013.
Goodwin, I.D., Browning, S.A., Mortlock, T., 2014. Eastern Australian Coastal Behaviour in Response to Extreme Storm Climate Between 1600–1900 AD, Determined from a Coupled Climate Reconstruction and Coastal Morphodynamic Approach. Abstract from American Geophysical Union Fall Meeting, San Francisco.
Guérin, G., Mercier, N., Adamiec, G., 2011. Dose-rate conversion factors: update. Ancient TL 29 (1), 5–8.
Harvey, N., Bourman, R.P., James, K., 2006. Evolution of the Younghusband Peninsula. South Australia: New Evidence from the Northern Tip. South Australian Geographical J. 105, 37–50.
Hesp, P.A., 1983. Morphodynamics of incipient foredunes in New South Wales. Australia. Developments in Sedimentology 38, 325–342. https://doi.org/10.1016/S0070-4571(08)70802-1.
Hesp, P.A., 1988a. Surfzone, beach and foredune interactions on the Australian south east coast. J. Coast. Res. SI 3, 15–25.
Hesp, P.A., 1988b. Morphology, dynamics and internal stratification of some established foredunes in southeast Australia. Sedim. Geol. 55 (1–2), 17–41. https://doi.org/10.1016/0037-0738(88)90088-7.
Hesp, P.A., 1989. A review of biological and geomorphological processes involved in the initiation and development of incipient foredunes. In: Gimingham, C.H., Ritchie, W., Willetts, B.B., Willis, A.J. (Eds.), Coastal Sand Dunes. Proc. Roy. Soc. Edinburgh Section B (Biol. Sci.). 96, pp. 181–202. https://doi.org/10.1017/S0269727000010927.
Hesp, P.A., 2002. Foredunes and Blowouts: initiation, geomorphology and dynamics. Geomorphology 48 (1–3), 245–268. https://doi.org/10.1016/S0169-555X(02)00184-8.
Hesp, P.A., 2013. Conceptual models of the evolution of transgressive dune field systems. Geomorphology 199, 138–149. https://doi.org/10.1016/j.geomorph.2013.05.014.
Hesp, P.A., Giannini, P.F.C., Martinho, C.T., Miot da Silva, G., Asp Neto, N.E., 2009. The Holocene Barrier Systems of the Santa Catarina Coast, Southern Brazil. In: Dillenburg, S. R., Hesp P.A. (Eds.), Geology and Geomorphology of Holocene Coastal Barriers of Brazil. Springer. Lect. Notes Earth Sci. 107, 93–133. https://doi.org/10.1007/978-3-540-44771-9_4.
Hill, P.J., Deckker, P.D., von der Borch, C., Murray-Wallace, C.V., 2009. Ancestral Murray River on the Lacepede Shelf, southern Australia: Late Quaternary migrations of a major river outlet and strandline development. Australian J. Earth Sciences 56, 135–157.
Hilton, M., Harvey, N., 2002. Management implications of exotic dune grasses on the Sir Richard Peninsula, South Australia. Proceedings of Coast to Coast. 2002. Australia's National Coastal Conference (Tweed Heads, New South Wales, Australia, pp. 186–189.
Hilton, M., Harvey, N., Hart, A., James, K., Arbuckle, C., 2006. The impact of exotic dune grass species on foredune development in Australia and New Zealand: a case study of Ammophila arenaria and Thinopyrum junceiforme. Aust. Geogr. 37 (3), 313–334. https://doi.org/10.1080/00049180600954765.
Huntley, D.J., Hutton, J.T., Prescott, J.R., 1994. Further thermoluminescence dates from the dune sequence in the south-east of South Australia. Quatern. Science Rev. 13 (3), 201–207. https://doi.org/10.1016/0277-3791(94)90025-6.
Kinsela, M.A., Daley, M.J.A., Cowell, P.J., 2016. Origins of Holocene coastal strandplains in Southeast Australia: shoreface sand supply driven by disequilibrium morphology. Mar. Geol. 374, 14–30. https://doi.org/10.1016/j.margeo.2016.01.010.
Lauzon, R., Murray, A.B., Moore, L.J., Walters, D.C., Kirwan, M.L., Fagherazzi, S., 2018. Effects of marsh edge erosion in coupled barrier island-marsh systems and geometric constraints on marsh evolution. J. Geophys. Res. Earth 123, 1218–1234. https://doi.org/10.1029/2017JF004530.
Leandro, C.G., Barboza, E.G., Caron, F., Jesus, F.A.N., 2019. GPR trace analysis for coastal depositional environments of southern Brazil. J. Appl. Geophys. 162, 1–12. https://doi.org/10.1016/j.jappgeo.2019.01.002.
Lewis, S.E., Sloss, C.R., Murray-Wallace, C.V., Woodroffe, C.D., Smithers, S.G., 2013. Post-glacial sea-level changes around the Australian margin: a review. Quatern. Science Rev. 74, 115–138. https://doi.org/10.1016/j.quascirev.2012.09.006.
Luebbers, R.A., 1978. Meals and menus: A study of change in prehistoric coastal settlements in South Australia (Unpublished Ph.D. thesis) (359 pp). Australian National University.
Luebbers, R.A., 1982. The Coorong Report. South Australia. Department of Environmental and Planning, Adelaide, Australia.
McKee, E.D., 1979. A Study of Global Sand Seas. United States Geol. Survey Prof. Paper 1052 Washington. DC. (429p).
McLean, R., Shen, J.S., 2006. From foreshore to foredune: foredune development over the last 30 years at Moruya Beach, New South Wales, Australia. J. Coast. Res. 22, 28–36. https://doi.org/10.2112/05A-0003.1.
Moore, L.J., List, J.H., Williams, S.J., Stolper, D., 2010. Complexities in barrier island response to sea-level rise: insights from model experiments, North Carolina Outer Banks. J. Geophys. Res. 115, 1–27. https://doi.org/10.1029/2009JF001299.
Morton, R.A., 1994. Texas Barriers. In: Davis Jr., R.A. (Ed.), Geology of Holocene Barrier Island Systems. Springer-Verlag, Berlin, pp. 75–114.
Moulton, M., Hesp, P.A., Miot da Silva, G., Bouchez, C., Lavy, M., Fernandez, G., 2018. Changes in vegetation cover on the Younghusband Peninsula transgressive dunefields (Australia) 1949–2017. Earth Surf. Process. Landforms 44, 459–470. https://doi.org/10.1002/esp.4508.
Murray, A.S., Wintle, A.G., 2003. The single aliquot regenerative dose protocol: potential for improvements in reliability. Radiat. Meas. 37 (4–5), 377–381. https://doi.org/10.1016/S1350-4487(03)00053-2.
Murray-Wallace, C.V., 2018. Quaternary History of the Coorong Coastal Plain. Springer, Southern Australia https://doi.org/10.1007/978-3-319-89342-6 229 p.
Murray-Wallace, C.V., Brooke, B.P., Cann, J.H., Belperio, A.P., Bourman, R.P., 2001. Whole-rock aminostratigraphy of the Coorong Coastal Plain, South Australia: towards a 1 million year record of sea-level highstands. J. Geol. Society 158, 111–124. https://doi.org/10.1144/jgs.158.1.111.
Murray-Wallace, C.V., Bourman, R.P., Prescott, J.R., Williams, F., Price, D.M., Belperio, A.P., 2010. Aminostratigraphy and thermoluminescence dating of coastal aeolianites and the later Quaternary history of a failed delta: the River Murray Mouth region, South Australia. Quatern. Geochron. 5 (1), 28–49. https://doi.org/10.1016/j.quageo.2009.09.011.

Neal, A., 2004. Ground-penetrating radar and its use in sedimentology: principles, problems and progress. Earth-Sci. Rev. 66, 261–330. https://doi.org/10.1016/j.earscirev.2004.01.004.

Oliver, T.S.N., Woodroffe, C.D., 2016. Chronology, morphology and GPR-imaged internal structure of the Callala Beach prograded barrier in southeastern Australia. J. Coast. Res. SI 75, 318–323. https://doi.org/10.2112/SI75-064.1.

Oliver, T.S.N., Dougherty, A.J., Gliganic, L.A., Woodroffe, C.D., 2014. Towards more robust chronologies of coastal progradation: Optically stimulated luminescence ages for the coastal plain at Moruya, south-eastern Australia. The Holocene 25, 536–546. https://doi.org/10.1177/0959683614561886.

Oliver, T.S.N., Tamura, T., Hudson, J.P., Woodroffe, C.D., 2017. Integrating millennial and interdecadal shoreline changes: Morpho-sedimentary investigation of two prograded barriers in southeastern Australia. Geomorphology 288, 129–147. https://doi.org/10.1016/j.geomorph.2017.03.019.

Oliver, T.S.N., Tamura, T., Short, A.D., Woodroffe, C.D., 2019a. Rapid shoreline progradation followed by vertical foredune building at Pedro Beach, southeastern Australia. Earth Surf. Process. Landforms 44, 655–666. https://doi.org/10.1002/esp.4510.

Oliver, T.S.N., Murray-Wallace, C.V., Woodroffe, C.D., 2019b. Holocene shoreline progradation and coastal evolution at Guichen and Rivoli Bays, southern Australia. The Holocene, 1–19 https://doi.org/10.1177/0959683619875815.

Ponder, W.F., Colgan, D.J., Clark, G.A., 1991. The morphology, taxonomy and genetic structure of Tatea (Mollusca: Gastropoda: Hydrobiidae), estuarine snails from temperate Australia. Australian J. of Zoology 39 (4), 447–497. https://doi.org/10.1071/ZO9910447.

Prescott, J.R., Hutton, J.T., 1994. Cosmic ray contributions to dose rates for luminescence and ESR dating: large depths and long-term time variations. Radiat. Meas. 23 (2–3), 497–500. https://doi.org/10.1016/1350-4487(94)90086-8.

Provis, D.G., Steedman, R.K., 1985. 1985. Wave measurements in the Great Australian Bight. Proc. Australasian Conf. Coastal Ocean Eng. Christchurch 2, 51–60.

Reimer, P.J., Bard, E., Bayliss, A., Beck, J.W., Blackwell, P.G., Bronk Ramsey, C., Buck, C.E., Cheng, H., Edwards, R.L., Friedrich, M., Grootes, P.M., Guilderson, T.P., Haflidason, H., Hajdas, I., Hatté, C., Heaton, T.J., Hoffmann, D.L., Hogg, A.G., Hughen, K.A., Kaiser, K. F., Kromer, B., Manning, S.W., Niu, M., Reimer, R.W., Richards, D.A., Scott, E.M., Southon, J.R., Staff, R.A., Turney, C.S.M., van der Plicht, J., 2013. Int Cal 13 and Marine 13 radiocarbon age calibration curves 0–50,000 years cal BP. Radiocarbon 55, 1869–1887. https://doi.org/10.2458/azu_js_rc.55.16947.

Reissen, A., Chappell, J.F., 1991. Murray Mouth Littoral Drift Study. Prepared for the Engineering and Water Supply Department of South Australia, 651–654.

Rodriguez, A.B., Meyer, C.T., 2006. Sea-level variation during the Holocene deduced from the morphologic and stratigraphic evolution of Morgan Peninsula, Alabama, U.S.A. J. Sedim. Res. 76 (2), 257–269. https://doi.org/10.2110/jsr.2006.018.

Roy, P.S., Thom, B.G., 1981. Late Quaternary marine deposition in New South Wales and southern Queensland – an evolutionary model. J. Geological Soc. Australia 28 (3–4), 471–489. https://doi.org/10.1080/00167618108729182.

Roy, P.S., Thom, B.G., Wright, L.D., 1980. Holocene sequences on an embayed high-energy coast: an evolutionary model. Sedim. Geol. 16 (1–3), 1–19. https://doi.org/10.1016/0037-0738(80)90003-2.

Roy, P.S., Cowell, P.J., Ferland, M.A., Thom, B.G., 1994. Wave-dominated coasts. In: Carter, R.W.G., Woodroffe, C.D. (Eds.), Coastal Evolution: Late Quaternary Shoreline Morphodynamics. Cambridge University Press, United Kingdom, pp. 121–186. https://doi.org/10.1017/CBO9780511564420.006.

Schwab, W.C., Thieler, E.R., Allen, J.R., Foster, D.S., Swift, B.A., Denny, J.F., 2000. Influence of inner-continental shelf geologic framework on the evolution and behavior of the barrier-island system between Fire Island Inlet and Shinnecock Inlet, Long Island, New York. J. Coast. Res. 16 (2), 408–422.

Shepherd, M.J., 1987. Sandy beach ridge system profiles as indicators of changing coastal processes. In New Zealand Geographical Society Conference Series 106–112.

Short, A.D., 1988. The South Australia coast and Holocene sea-level transgression. Geogr. Rev. 78, 119–136. https://doi.org/10.2307/214171.

Short, A.D., Hesp, P.A., 1982. Waves beach and dune interactions in southeastern Australia. Mar. Geol. 48 (3–4), 259–284. https://doi.org/10.1016/0025-3227(82)90100-1.

Short, A.D., Hesp, P.A., 1984. Beach and Dune Morphodynamics of the southeast coast of South Australia. Tech. Rept. 84/1. Coastal Studies Unit, Dept. Geography, Univ. Sydney, 142pp.

Short, A.D., Woodroffe, C.D., 2009. The Coast of Australia. Cambridge University Press https://doi.org/10.1111/j.1745-5871.2009.00633.x 288 p.

Stolper, D., List, J.H., Thieler, E.R., 2005. Simulating the evolution of coastal morphology and stratigraphy with a new morphological-behaviour model (GEOMBEST). Mar. Geol. 218, 17–36. https://doi.org/10.1016/j.margeo.2005.02.019.

Tamura, T., 2012. Beach ridges and prograded beach deposits as palaeoenvironment records. Earth-Sci. Rev. 114 (3–4), 279–297. https://doi.org/10.1016/j.earscirev.2012.06.004.

Thom, B.G., 1984. Transgressive and regressive stratigraphies of coastal sand barriers in southeast Australia. Mar. Geol. 56 (1–4), 137–158. https://doi.org/10.1016/0025-3227(84)90010-0.

Thom, B.G., Roy, P.S., 1985. Relative sea levels and coastal sedimentation in southeast Australia in the Holocene. J. Sediment. Petrol. 55 (2), 257–264. https://doi.org/10.1306/212F8693-2B24-11D7-8648000102C1865D.

Thom, B.G., Bowman, G.M., Gillespie, R., Polach, H.A., Barbetti, M., 1981. Progradation histories of sand barriers in New South Wales. Search 12, 323–325.

Thom, B.G., Shepherd, M., Ly, C.K., Roy, P.S., Bowman, G.M., Hesp. P.A., 1992. Coastal geomorphology and Quaternary geology of the Port Stephens-Myal Lakes area. Canberra: Department of Biogeography and Geomorphology. The Australian National University, 407 p.

Timmons, E.A., Rodriguez, A.B., Matheus, C.R., DeWitt, R., 2010. Transition of a regressive to a transgressive barrier island due to back-barrier erosion, increased storminess, and low sediment supply: Bogue Banks, North Carolina, USA. Mar. Geol. 278(1–4), 100–114. doi:https://doi.org/10.1016/j.margeo.2010.09.006.

Walters, D., Moore, L.J., Vinent, O.D., Fagherazzi, S., Mariotti, G., 2014. Interactions between barrier islands and backbarrier marshes affect island system response to sea level rise: insights from a coupled model. Journal of Geophysical Research Earth Surface 119, 2013–2031. https://doi.org/10.1002/2014JF003091.

Wright, L.D., 1976. Nearshore wave-power dissipation and the coastal energy regime of the Sydney-Jervis Bay region, New South Wales: a comparison. Austral. J. Marine and Freshwater Resources 27, 633–640. https://doi.org/10.1071/MF9760633.